Excitation of Toroidicity-Induced Alfvén Eigenmodes by the Electrodes Inserted in a Heliotron/Torsatron Plasma

G. Matsunaga,[1,*] K. Toi,[2] S. Kawada,[1] J. Kotani,[1] C. Suzuki,[2] K. Matsuoka,[2] and CHS Group[2]

[1]*Department of Energy and Engineering Science, Nagoya University, Nagoya 464-8601, Japan*

[2]*National Institute for Fusion Science, Toki 509-5292, Japan*

(Received 30 September 2002; published 9 June 2005)

A novel method of exciting shear Alfvén waves using electrodes inserted in a plasma was developed for basic study of Alfvén eigenmodes in a heliotron/torsatron plasma. The electrodes can induce excitation current along the confinement field line, and generate magnetic perturbations perpendicular to the confinement field. By sweeping the frequency of the current in a cold plasma, the toroidicity-induced Alfvén eigenmode was resonantly excited at the predicted frequency and radial location. Plasma response to the applied magnetic perturbations indicates a fairly large damping rate caused by continuum damping.

DOI: 10.1103/PhysRevLett.94.225005 PACS numbers: 52.35.Bj, 52.55.Hc, 52.55.Pi

Energetic alpha particles in a fusion plasma could excite Alfvén eigenmodes (AEs) and in turn they would degrade the confinement and lead to the quenching of deuterium-tritium (DT) ignition. Stability of AEs such as toroidicity-induced AEs (TAEs) is intensively studied using energetic ions produced by neutral beam injection and so on, in major tokamaks [1] and helical devices [2–4]. The stability of energetic-ion driven AEs is determined through competition between the energetic-ion drive and various damping mechanisms. Electron and ion Landau damping are well documented. Continuum damping occurs as the resonant power absorption when the eigenfrequency intersects with a shear Alfvén continuum. This damping essentially depends on the radial profiles of the global magnetic shear $s(=(r/q)dq/dr)$, where q is the safety factor and r is the minor radius [5,6]. It is expected that the continuum damping is strong on a helical device such as the heliotron/torsatron, which has negative and strong magnetic shear $|s| > 1$ at the plasma edge, compared with a tokamak device. Radiative damping takes place within the gap region through mode coupling between AE and kinetic Alfvén wave, by which mechanisms the wave energy of AE is transferred to the plasma core region from the gap region [7,8]. Note that the radiative damping is effective under $k_\perp \rho_s \geq 1$, where $k_\perp$ and ρ_s are the wave number perpendicular to the magnetic field and the ion Larmor radius evaluated with the electron temperature. Although these damping mechanisms are though to play an important role in a fusion plasma, comparison between experiments and theories is insufficient.

In the CHS heliotron/torsatron with poloidal and toroidal field periods $l = 2$ and $N = 8$, of which major and minor radii are $R \simeq 1$ m and $\langle a \rangle \simeq 0.2$ m, respectively [9], we have carried out AE experiments on a special plasma condition, that is, in a very low beta (= plasma pressure/magnetic pressure) plasma with low temperature and low density. Thus low beta plasma without energetic ions provides a simple and useful opportunity for a basic study of AEs focusing on continuum and radiative damping, because electron and ion Landau damping can be neglected in the plasma condition. In addition, detailed internal information of AE fluctuations can easily be obtained by insertion of a magnetic probe array and Langmuir probes. It should be noted that the eigenfrequency, mode structure, and continuum damping of AEs do not depend upon plasma temperature. Therefore, the experimental results obtained in cold plasma can be projected to those in high temperature plasma. In the JET tokamak, AEs are successfully excited without energetic ions by using a set of saddle coils installed inside the vacuum vessel, and the damping rate is experimentally evaluated from the plasma response to applied magnetic field perturbations [10]. Thus the measured damping rate clearly depends on the magnetic shear and the plasma shaping.

In the CHS experiment, we have developed a novel technique to excite shear Alfvén perturbations effectively instead of using a similar coil system to that in JET,

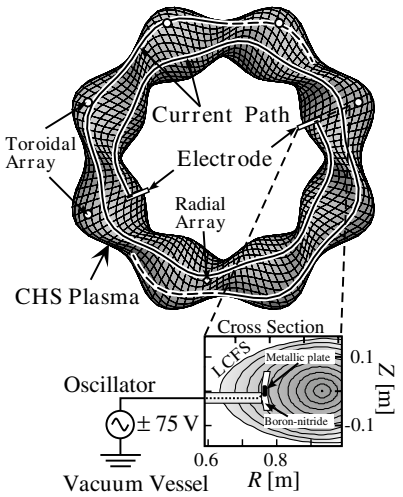

FIG. 1. Schematic drawing of electrode system and poloidal cross section with a simplified electrical circuit in a CHS plasma. The current paths along the confinement field line are drawn as bold lines from electrodes.

because the CHS has a three-dimensional and complex magnetic configuration and it is very difficult to excite shear Alfvén waves minimizing the perturbations parallel to the confinement field. Moreover, the rotational transform $\iota(=1/q)$ in CHS is an increasing function of the minor radius r, that is, negative and strong magnetic shear, such as $s \sim -4$. This leads to the TAE gap frequency rapidly increasing toward the edge. Therefore, the excitation system is required to overcome the strong continuum damping near the edge. The newly developed excitation system is composed of two insertable electrodes that are arranged 180 degrees apart in the toroidal direction to specify the toroidal mode number, as shown in Fig. 1. The electrode has a metallic plate of 30 mm $\times$ 10 mm size perpendicular to the magnetic field line. One side of the metallic plate is insulated with a block of boron nitride to specify the path of oscillatory current in the one toroidal direction. The most significant point of this system is that magnetic perturbations induced by the oscillatory current are perpendicular to the equilibrium magnetic field, and would generate shear Alfvén waves very effectively. Moreover, these electrodes can be inserted into a plasma core region up to the normalized radial position $\rho(= r/\langle a\rangle) \simeq 0.65$. It is expected that the effect of continuum damping near the edge would be minimized by placing the electrodes beyond the edge ($\rho > 0.8$). The predicted current path generated by this system and the simplified electrical circuit for excitation are also shown in Fig. 1, together with the locations of magnetic probe arrays.

In this experiment, the electrodes were inserted inside beyond the last closed flux surface (LCFS) up to $\rho \simeq 0.65$ in a low density and low temperature helium plasma. The plasma has been produced with 2.45 GHz electron cyclotron waves (ECWs) up to 1 kW at low magnetic field (~ 0.09 T) on the magnetic axis. The electron density and electron temperature of the plasma are in the range of $\sim 3 \times 10^{16}$ m^{-3} and ~ 4 eV, respectively. These typical profiles measured with a triple probe are shown in Fig. 2. In this plasma, the expected TAE gap frequency and position are in the range of 50 kHz to 300 kHz and $\rho \leq 0.8$, respectively. When oscillatory voltage in the range of 100 kHz is applied between each electrode and the vacuum vessel wall, the oscillatory current is induced along a specified magnetic field line as an electron or ion saturation current, depending on the polarity of the applied voltage. That is, each electrode acts as a single Langmuir probe. The peak voltage applied to each electrode is ± 75 V, and the electron saturation current reaches in the order of 200 mA. The length of the current path along the equilibrium magnetic field line is determined by a so-called free streaming length, which is determined by the balance between the particle fluxes parallel and perpendicular to the magnetic field line [11]. In this plasma, the length of electron is about 5 m. When the electrodes are placed at $\rho \simeq 0.65$, the oscillatory current will flow on the magnetic field line that is on the magnetic surface of $\iota \simeq 1/2$. Accordingly, the generated dominant Fourier mode is $m/n = 4/2$ and the sideband of $m \pm 1$ mode components will also be generated through the toroidal effect.

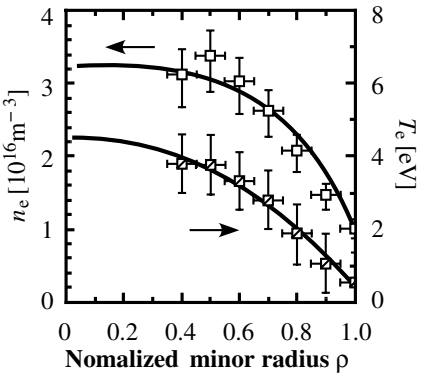

FIG. 2. Radial profiles of electron density and electron temperature of a plasma produced by 2.45 GHz ECW.

A resonance character in a plasma response to the applied magnetic perturbations is successfully derived from the transfer function defined as $G(f_{ex}) = b(f_{ex})/I_0(f_{ex})$, where $b(f_{ex})$, $I_0(f_{ex})$ and f_{ex} are the Fourier transforms of magnetic field fluctuations excited in a plasma, oscillatory current induced by electrodes and the exciting frequency, respectively. The response magnetic field fluctuations $b(t)$ are directly measured using magnetic probe arrays inserted into plasma. Because levels of these signals are lager than noise ones, a synchronous detector is not used in this experiment. When the frequency of the current is swept around the TAE gap frequency f_{TAE}, the poloidal component of the transfer function $G_\theta(f_{ex})$ would exhibit a character of resonance behavior related to f_{TAE}. An example of the transfer function obtained in this experiment is shown in Fig. 3, where the frequency is swept around 200 kHz in a quasistationary plasma phase and the electrodes are placed at $\rho \simeq 0.65$ near the relevant TAE gap. In Fig. 3(a), the absolute value $|G_\theta|$, real part Re$[G_\theta]$, and

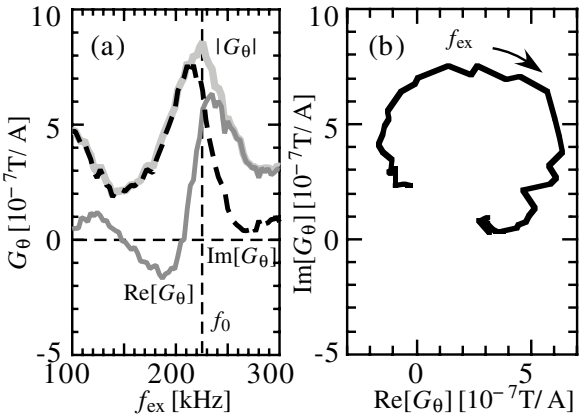

FIG. 3. Example of plasma response, which is the transfer function for induced magnetic perturbations. (a) The absolute $|G_\theta|$, the real part Re$[G_\theta]$, and the imaginary part Im$[G_\theta]$ of the poloidal component of the transfer function G_θ. (b) Transfer function in the complex plane.

imaginary one $\mathrm{Im}[G_\theta]$ are shown for an enlarged frequency around f_{TAE}. The transfer function draws a circle in the complex plane across the resonance frequency f_0, as shown in Fig. 3(b). The toroidal mode of the induced magnetic fluctuations was derived as $n = 2$ from the toroidal array of magnetic probes. It should be noted that the polarity of the oscillatory current for each two electrodes is adjusted to excite an even pattern of perturbations. Plasma parameters related to the Alfvén velocity, that is, the toroidal field B_t, the electron density n_e, and the mass of the fuel ion A_i, are varied in order to confirm that this resonance is related to TAEs. Figure 4 indicates the relationship between the observed resonance frequency f_0 and the calculated TAE gap frequency $f_{\mathrm{cal}} = [v_A \iota/(4\pi R)]_{\rho=\rho_0}$, where v_A is the Alfvén velocity. Here, f_{cal} was evaluated as that of the TAE gap formed at $\rho = \rho_0 \simeq 0.5$ by the mode coupling of $m = 4$ and $m = 5$ poloidal modes, where $\iota(\rho_0) = 0.44$. This figure clearly indicates that the resonance is related to TAEs.

In an ECW plasma without fast ions, the effective damping rate $\gamma_{\mathrm{eff}} (= \gamma_d - \gamma_f)$ is equivalent to the damping rate γ_d because the fast ion drive γ_f is zero. Therefore, the damping rate is evaluated from the shape of the transfer function $|G_\theta|$ shown in Fig. 3 together with the resonance frequency $f_{\mathrm{ex}} = f_0$. That is, $\gamma_d^{\mathrm{exp}}/\omega_0 \propto \Delta f/f_0$, where Δf is the full width at half maximum of the resonance peak and $\omega_0 = 2\pi f_0$. The damping rate derived from the data such as Fig. 3 is fairly large to be $\gamma_d^{\mathrm{exp}}/\omega_0 \sim 10\%$ as shown in Fig. 4(b).

It is important and interesting to measure the internal structure of AEs [12]. In this experiment, a radial array of magnetic probes was inserted to measure the radial profile of magnetic fluctuations induced by the electrode system. Three components of magnetic fluctuations, b_r, b_θ, and b_ϕ, were measured simultaneously at 24 radial positions by this radial array. In this experiment, a radial profile of the transfer function $|G|$ at $f_{\mathrm{ex}} = f_0$ is shown in Fig. 5. The toroidal component of the transfer function $|G_\phi|$ is much smaller than the radial $|G_r|$ and poloidal $|G_\theta|$ components, as shown in Fig. 5(a). This clearly indicates that the induced magnetic fluctuations have a character of shear Alfvén waves. However, we speculate that a finite $|G_\phi|$ in the core region shows the possibility of exciting a compressional Alfvén wave.

The magnitude of $|G_\theta|$ has two peaks around $\rho \sim 0.2$ and $\rho \sim 0.7$, and the phase of the transfer function $\angle G_\theta$ is inverted at $\rho \sim 0.5$ [Fig. 5(b)]. The radial displacement of TAE may roughly be derived from the data shown in Fig. 5. The magnetic perturbation vector $\boldsymbol{b}$ will be related to the plasma displacement vector ξ through $\boldsymbol{b} = \nabla \times (\xi \times \boldsymbol{B_0})$, where $\boldsymbol{B_0}$ is the vector of the equilibrium magnetic field. If a cylindrical configuration is assumed for simplicity, the radial displacement ξ_r is evaluated as $\xi_r \simeq -\frac{1}{B_\theta} \times \int_0^r b_\theta dr' \propto \int_0^r G_\theta dr'$, where B_θ is the poloidal magnetic field, the magnitude and phase of G_θ are taken into account. The spatial integration of G_θ is shown in Fig. 5(c). This indicates that the eigenmode has a peak in the radial location of $\rho \simeq 0.4$–0.6. The difference in the radial integrations of imaginary and real parts of G_θ is thought to be due to the above simplified calculation. It is interesting to compare the experimental results with the shear Alfvén continua calculated on the assumption of an axisymmetric configuration such as a tokamak [13]. In Fig. 6(a), the $n = 2$ shear Alfvén continua are shown for a helium plasma obtained by 2.45 GHz ECW, where a singly ionized helium plasma is assumed because of low T_e as shown in Fig. 2 and the ion density profile is assumed to be the same profile shape of electron density in Fig. 2. Here, the rotational

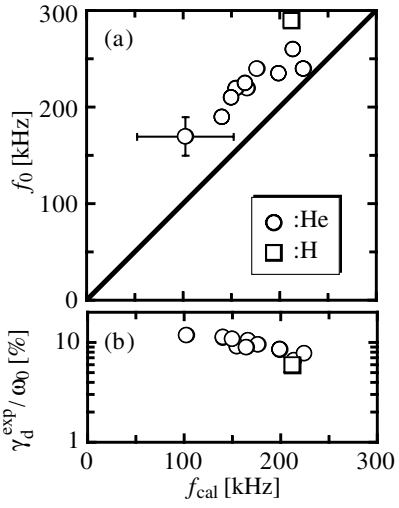

FIG. 4. Observed resonance frequency and damping rate of excited TAEs for several experimental conditions. Open circles and squares show helium and hydrogen experimental results, respectively.

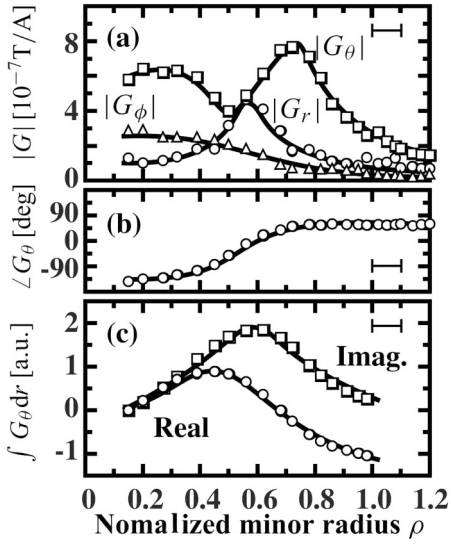

FIG. 5. Radial profiles of the transfer function. (a) The absolute value of transfer functions for three field components, (b) the phase for G_θ and (c) the effective eigenfunction evaluated as $\int G_\theta dr$.

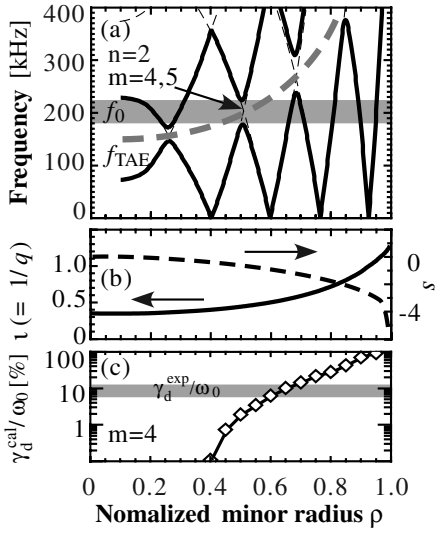

FIG. 6. (a) Calculated Alfvén continua for $n = 2$ in a helium plasma produced by 2.45 GHz ECW. (b) Radial profiles of rotational transform and magnetic shear in CHS. (c) Calculated continuum damping rate by Ref. [5], together with measured one (horizontal zone).

transform profile in the $R_{ax} = 97.4$ cm magnetic configuration of zero plasma pressure is adopted [Fig. 6(b)]. The eigenfrequency obtained with the electrode technique is indicated by the gray zone and agrees well with the TAE gap generated by $m = 4$ and $m = 5$ poloidal mode coupling. If the eigenfunction extends as shown in Fig. 5(c), the excited $n = 2$ TAE would suffer from considerable continuum damping in the edge region outside the relevant TAE gap, i.e., $\rho \sim 0.65$.

As mentioned above, electron and ion Landau damping can be neglected because electron and ion pressures are very low in the present plasma condition. In this plasma, the ionization degree is fairly low, that is, only ~25%. That is, the neutral density is in the order of $\sim 10^{17}$ m^{-3}, and the collision frequency of electrons with neutrals is about 10 kHz. This neutral effect on the damping rate, however, is negligibly small [14]. It is expected that the radiative damping is less effective in this low temperature plasma, because $k_\perp \rho_s \leq 1$ and $v_e < v_A$, where v_e is the electron thermal velocity. To make sure this expectation is realized, the mass of ion m_i was changed because the radiative damping is proportional to $\sqrt[3]{m_i}$. However, the damping rates for these gases are almost same in spite of changing the ion mass, as seen from Fig. 4(b). It is thought that radiative damping will not be the case in the present plasma condition. As shown in Fig. 6(b), the magnetic shear is high, that is, $s < -1$ in the region of $\rho > 0.7$. If the eigenfunction of this mode expands to the edge region, it will suffer from fairly large continuum damping. The damping rate estimated by the equation in Ref. [5] is considerably large (~20%) as shown in Fig. 6(c). This shows that experimental results are consistent with theoretical value and the continuum damping is dominant in this plasma condition.

In conclusion, we have developed a novel electrode technique that can effectively excite shear Alfvén waves. In this experiment, the eigenfrequency and damping rate of the excited TAE were successfully derived from the resonant character of the transfer function G_θ. The frequency agrees well with the $n = 2$ TAE gap frequency related to $m = 4$ and $m = 5$ mode coupling. The derived damping rate of ~(5–10)% is thought to be dominated by continuum damping. Moreover, this experimental technique may be extended for the investigation of radiative damping as well as continuum damping in high density helium or neon plasmas produced by whistler wave and electron Bernstein waves under $v_e > v_A$ [15,16]. Therefore, the basic study of continuum and radiative damping can easily be carried out by changing the electron density and/or ion mass. Application of this newly developed electrode technique to a low temperature and low density plasma will make the detailed investigation of the excitation and damping of AEs easier in three-dimensional magnetic configurations such as various types of stellarators.

This work was supported in part by the Grant-in-Aid for Scientific Research from Japan Society for the Promotion of Science, No. 12480127 and No. 16082209.

*Electronic address: matunaga@fusion.naka.jaeri.go.jp

[1] K. L. Wong, Plasma Phys. Controlled Fusion **41**, R1 (1999).
[2] A. Weller *et al.*, Phys. Plasmas **8**, 931 (2001).
[3] M. Takechi *et al.*, Phys. Rev. Lett. **83**, 312 (1999).
[4] K. Toi *et al.*, Nucl. Fusion **40**, 1349 (2000).
[5] M. N. Rosenbluth, H. L. Berk, J. W. Van Dam, and D. M. Lindberg, Phys. Rev. Lett. **68**, 596 (1992).
[6] F. Zonca and L. Chen, Phys. Rev. Lett. **68**, 592 (1992).
[7] R. R. Mett and S. M. Mahajan, Phys. Fluids B **4**, 2885 (1992).
[8] A. Jaun *et al.*, Phys. Plasmas **5**, 2952 (1998).
[9] K. Matsuoka *et al.*, in *Plasma Physics and Controlled Nuclear Fusion Research 1988: Proceedings of the 12th IAEA Conference Nice, 1988* (IAEA, Vienna, 1989), Vol. 2, p. 411.
[10] A. Fasoli *et al.*, Phys. Rev. Lett. **75**, 645 (1995).
[11] S. A. Cohen *et al.*, J. Nucl. Mater. **76–77**, 68 (1978).
[12] T. E. Evans *et al.*, Phys. Rev. Lett. **53**, 1743 (1984).
[13] C. Z. Cheng and M. S. Chance, Phys. Fluids **29**, 3695 (1986).
[14] Y. Amagishi and A. Tsushima, Plasma Phys. Controlled Fusion **26**, 1489 (1984).
[15] R. Ikeda *et al.*, in *Proceedings of the 12th International Congress on Plasma Physics, Nice, 2004.*
[16] T. Shoji *et al.*, in *Proceedings of the 12th International Congress on Plasma Physics, Nice, 2004.*